AFRL-RY-WP-TR-2019-0076

ELECTRON DRIFT MOBILITY OF DEGENERATE SEMICONDUCTORS DUE TO IONIZED IMPURITY SCATTERING – PHASE II

Daniel Rode

Pendragon Corporation

APRIL 2019
Final Report

AIR FORCE RESEARCH LABORATORY
SENSORS DIRECTORATE
WRIGHT-PATTERSON AIR FORCE BASE, OH 45433-7320
AIR FORCE MATERIEL COMMAND
UNITED STATES AIR FORCE

NOTICE AND SIGNATURE PAGE

Using Government drawings, specifications, or other data included in this document for any purpose other than Government procurement does not in any way obligate the U.S. Government. The fact that the Government formulated or supplied the drawings, specifications, or other data does not license the holder or any other person or corporation; or convey any rights or permission to manufacture, use, or sell any patented invention that may relate to them.

This report is the result of contracted fundamental research deemed exempt from public affairs security and policy review in accordance with SAF/AQR memorandum dated 10 Dec 08 and AFRL/CA policy clarification memorandum dated 16 Jan 09. This report is available to the general public, including foreign nationals.

Copies may be obtained from the Defense Technical Information Center (DTIC) (http://www.dtic.mil).

AFRL-RY-WP-TR-2019-0076 HAS BEEN REVIEWED AND IS APPROVED FOR PUBLICATION IN ACCORDANCE WITH ASSIGNED DISTRIBUTION STATEMENT.

// Signature//	// Signature//
JOHN S. CETNAR, Program Manager	ROSS W. DETTMER, Branch Chief
Electronic Devices Branch	Electronic Devices Branch
Aerospace Components & Subsystems Division	Aerospace Components & Subsystems Division

This report is published in the interest of scientific and technical information exchange, and its publication does not constitute the Government's approval or disapproval of its ideas or findings.

*Disseminated copies will show "//Signature//" stamped or typed above the signature blocks.

REPORT DOCUMENTATION PAGE

Form Approved
OMB No. 0704-0188

1. REPORT DATE *(DD-MM-YY)*	2. REPORT TYPE	3. DATES COVERED *(From - To)*
April 2019	Final	6 September 2018 – 26 October 2018

4. TITLE AND SUBTITLE
ELECTRON DRIFT MOBILITY OF DEGENERATE SEMICONDUCTORS DUE TO IONIZED IMPURITY SCATTERING – PHASE II

5a. CONTRACT NUMBER
N/A

5b. GRANT NUMBER

5c. PROGRAM ELEMENT NUMBER
N/A

6. AUTHOR(S)
Daniel Rode

5d. PROJECT NUMBER
N/A

5e. TASK NUMBER
N/A

5f. WORK UNIT NUMBER
N/A

7. PERFORMING ORGANIZATION NAME(S) AND ADDRESS(ES)
Pendragon Corporation
19390 Collins Avenue, Unit 1116
Sunny Isles Beach, FL 33160

8. PERFORMING ORGANIZATION REPORT NUMBER
AFRL-RY-WP-TR-2019-0076

9. SPONSORING/MONITORING AGENCY NAME(S) AND ADDRESS(ES)
Air Force Research Laboratory
Sensors Directorate
Wright-Patterson Air Force Base, OH 45433-7320
Air Force Materiel Command
United States Air Force

Air Force Office of Scientific Research (AFOSR)
875 North Randolph Street, Suite 325, Room 3112
Arlington, VA 22203

10. SPONSORING/MONITORING AGENCY ACRONYM(S)
AFRL/RYDD

11. SPONSORING/MONITORING AGENCY REPORT NUMBER(S)
AFRL-RY-WP-TR-2019-0076

12. DISTRIBUTION/AVAILABILITY STATEMENT
Approved for public release; distribution is unlimited.

13. SUPPLEMENTARY NOTES
PAO case number 88ABW-2019-0678, Clearance Date 19 February 2019. Also see AFRL-RY-WP-TR-2019-0075 and AFRL-RY-WP-TR-2019-0077. Report contains color.

14. ABSTRACT
Analysis of electron mobility due to ionized impurity scattering for degenerate semiconductors and verification of electron mobility equations.

15. SUBJECT TERMS
degenerate semiconductors, ionized impurity scattering, non-parabolic conduction bands

16. SECURITY CLASSIFICATION OF:			17. LIMITATION OF ABSTRACT:	18. NUMBER OF PAGES	19a. NAME OF RESPONSIBLE PERSON (Monitor)
a. REPORT	b. ABSTRACT	c. THIS PAGE			John Cetnar
Unclassified	Unclassified	Unclassified	SAR	24	19b. TELEPHONE NUMBER *(Include Area Code)* N/A

Table of Contents

Section **Page**

List of Figures

Figure **Page**

List of Tables

Table **Page**

1. Objective

In the initial phase of this work, a recently developed theory of electron transport for heavily doped, degenerate semiconductors was introduced.[1] Since there is no previously existing equivalent theory with which to make comparisons in order to verify the accuracy of the new formulation, it is imperative to identify whatever other methods can be found by which such comparisons and verifications can be made.

Thus, the major objective of this work is to verify the accuracy of the newly developed analytical expressions for the electron mobility of degenerate semiconductors dominated by ionized impurities, including non-parabolic conduction bands and wave function admixtures. Three methods are to be used; *i)* ensure exact agreement with prior theory in the asymptotic limit of parabolic conduction bands, *ii)* numerical integration by quadrature of formulas and comparison to results from exact analytical expressions, and, *iii)* comparisons of computed numerical results using various formulas.

2. Motivation

The classical theoretical treatment of the electron mobility of degenerate semiconductors is based on parabolic conduction bands and Thomas-Fermi screening. The corresponding results can be significantly in error (by about fifty to one-hundred percent) in comparison to experiments. In order to explain experimental results with accuracy within a few percent, it is necessary to incorporate non-parabolicity of the conduction band into the theory. However, when the conduction band is non-parabolic, the electron wave functions necessarily consist of a mixture of *s* and *p* wave functions, the so-called basis functions. Because the basis functions are orthogonal, the strength of electron scattering is consequently *decreased*. On the other hand, conduction band non- parabolicity causes *increased* electron scattering. To quantitatively characterize these variations, one must have recourse to the full theoretical treatment introduced earlier for electron transport and electron mobility.[1]

Therefore, it is the purpose of this work to verify the accuracy of the new theory to within a few percent.

3. Fundamental Equations

3.1 Band Structure

Students of physics are familiar with the concept of kinetic energy, which varies parabolically with either velocity *v* or momentum *p*.

$$K.E. = mv^2/2 = p^2/2m \tag{1}$$

Of course, this concept usually assumes constancy of the quantity "m," called mass. While this assumption may be accurate for the small velocities associated with celestial bodies such as the moons and planets of the Solar system, which were of concern to Newton, it is not true for relativistic velocities; and it certainly is not true for electrons in heavily doped (*i.e.* degenerate) semiconductors. These three cases are represented graphically in Figure 1.

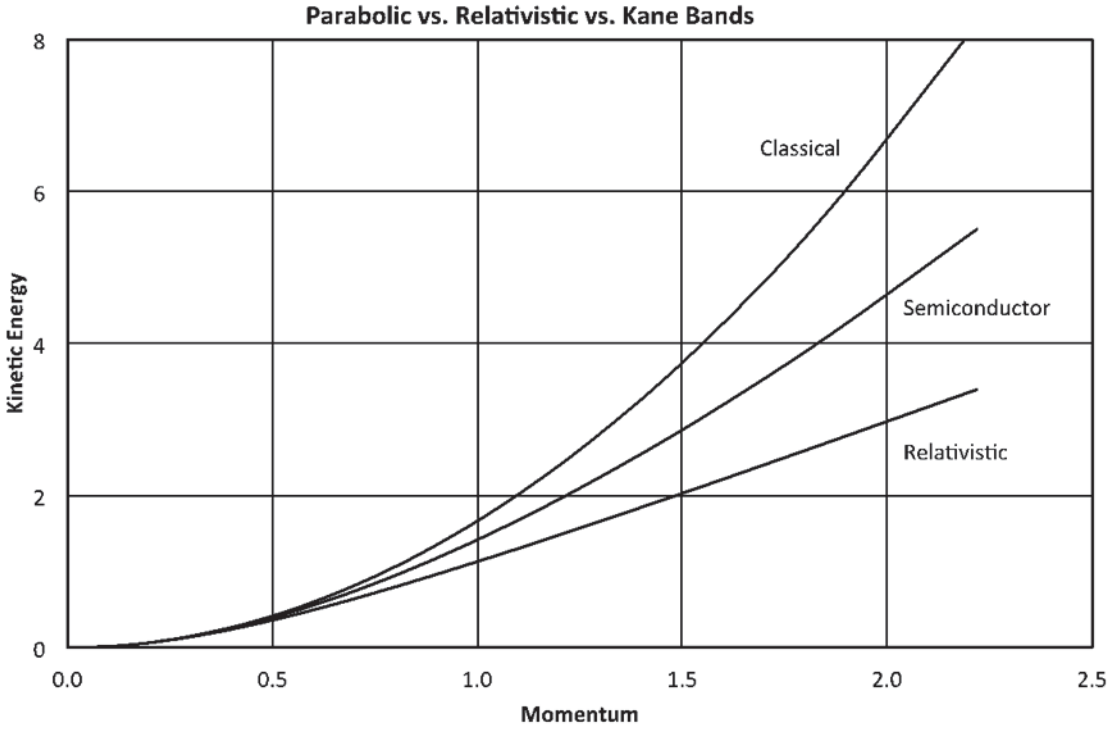

Figure 1: Classical, Semiconductor, and Relativistic Dispersion Relations Compared

The assumed mass is the same for all three cases: *i)* the Classical case of eq. (1), *ii)* the Relativistic case of Einstein where

$$K.E. = \sqrt{(cp^2)^2 + (mc^2)^2} - mc^2 \tag{2}$$

and *iii)* the case of electrons in semiconductors where the conduction band is adapted from the work of Kane[2] by Rode.[3]

$$E = E_o - \frac{E_g}{2}\left[1 - \sqrt{1 + 4E_o\left(\frac{m}{m^*} - 1\right)/E_g}\right] \tag{3}$$

Here, *Eg* is the energy gap, *m** is the effective mass given by the reciprocal of the curvature at the bottom of the conduction band, and the magnitude of the electron wave vector is *k*.

$$m^* = 1/(\partial^2 E/\partial p^2) \tag{4}$$

The free-electron energy is given in terms of the free-electron mass *m*. The distinction is made throughout this work between *free* electrons and *conduction* electrons; consequently, *m* is the rest mass of a free electron in vacuum whereas a conduction electron may possess an effective mass *m**. Thus,

$$E_o = \hbar^2 k^2/2m = p^2/2m \tag{5}$$

It can be clearly seen in Figure 1 that, except for "classical" particles, the kinetic energy varies sub-parabolically with momentum. This result is sometimes represented by the suggestion that the mass is not constant but, rather, increases with momentum (see Appendix A).

Instead, throughout the present work, the point of view will be taken that the proper way to describe the kinematics of electrons in semiconductors is by specifying their energy versus momentum relationship *E(p)* or *E(k)*. Furthermore, this so-called dispersion relation *E(k)* for semiconductors will be taken to be given by eq. (3).

When the conduction band is non-parabolic, as it is for eq. (3), the electron wave function necessarily consists of an admixture of both *s* and *p*-type basis functions.[3]

$$\vartheta_{k\beta} = a[iS\downarrow] + c[Z\downarrow] \tag{6}$$

For classical parabolic bands, *c* vanishes and the magnitude of *a* is equal to unity. In general,

$$a^2 + c^2 = 1 \tag{7}$$

$$c^2 = 1/2 - 1/2\sqrt{1 + 2\hbar^2 k^2 (m/m^* - 1)/mE_g} \tag{8}$$

Typical values of *c*2 are shown in Figure 2. For degenerate semiconductors of interest for the present work where 5% theoretical precision is required, wave function admixture is important when the electron concentration exceeds about 10^{20}/cc.

Note that the effect of wave function admixture is to decrease the frequency of electron scattering because of the orthogonality of *s* and *p*-type basis functions and, hence, the electron mobility is *increased*. On the other hand, the effect of conduction band non- parabolicity is to *decrease* the electron mobility because of the increased effective mass. Typically, the admixture

effect is dominant (see Appendix B).

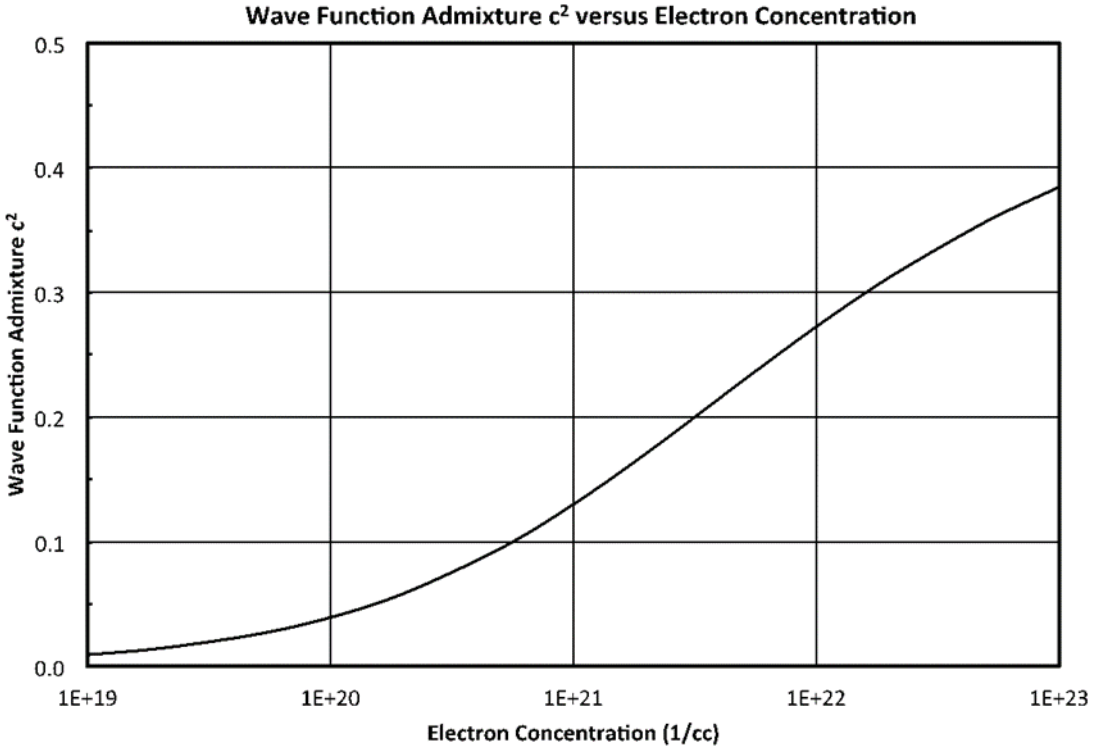

Figure 2: Wave Function Admixture is Significant for Degenerate Semiconductors with Conduction Electron Concentration in Excess of about 10^{20}/cc

3.2 Parabolic Limits of Band Structure Equations

The major objective of the present Phase II work is to verify the accuracy of newly developed equations appearing in Phase I work. Of the three methods of verification, one involves the use of parabolic limits to the equations so that direct comparisons can be made to pre-existing work found in textbooks and scientific journals.[4,5] The second and third methods rely on numerical integration, and comparisons between numerical computations.

Eq. (1) is, of course, the classical parabolic expression for kinetic energy, but concern here is with eq. (3) for Kane bands, which will be used below for degenerate semiconductors. From eq. (3), in the limit of large energy gap,

$$E \to E_o - \frac{E_g}{2}\left[1 - 1 - 2E_o\left(\frac{m}{m^*} - 1\right)/E_g\right]$$

$$E \to E_o + E_o\left(\frac{m}{m^*} - 1\right)$$

$$E \to mE_o/m^* = \hbar^2 k^2/2m^*$$

$$E \to E_{parabolic} = \hbar^2 k^2/2m^* \qquad (9)$$

Therefore, parabolic bands result in the limit of large energy gap. This limit will be used to test several equations in the work that follows. For example, equations (7) and (8) show that the magnitude of *a* is equal to unity and *c* vanishes in the limit of large energy gap, *i.e.* for parabolic bands.

3.3 Electron Probability Distribution and Fermi Level

Because electrons are odd half-integer spin particles, they obey the Pauli Exclusion Principle and the Fermi-Dirac probability distribution function *f* where E_F is the Fermi Level. (Alternatively, even half-integer spin particles such as photons obey the Bose-Einstein probability distribution function.)

$$f = \frac{1}{1+e^{(E-E_F)/\kappa T}} \tag{10}$$

The density-of-states function in *k*-space is $(k/\pi)^2$. Therefore, the concentration of conduction electrons is equal to the sum over occupied states ranging over *k*-space.

$$n = \int \left(\frac{k}{\pi}\right)^2 f\, dk \tag{11}$$

When non-degenerate conditions prevail, *f* is small in comparison to unity and the usual textbook result obtains where N_c is the thermal density-of-states, also known as the effective density of states. When the Fermi Level lies at the conduction band edge where E_F equals zero, the electron concentration equals N_c.

$$n = N_c e^{E_F/\kappa T} \tag{12}$$

This case is of no further concern here. On the other hand, for degenerate conditions where $E_F/\kappa T >> 1$, the probability distribution function *f* is essentially equal to unity for *k* values ranging from zero up to the Fermi Level where $k = k_F$. Integration of eq. (11) gives

$$n = k_F^3/3\pi^2 \tag{13}$$

Combining equations (3) and (13) gives the Fermi Level in terms of the conduction electron concentration for non-parabolic bands, which expression is necessary for mobility calculations later on.

$$E_F = \frac{(3\pi^2 n)^{2/3}\hbar^2}{2m} - \frac{E_g}{2}\left[1 - \sqrt{1 + 2\hbar^2(3\pi^2 n)^{2/3}(1/m^* - 1/m)/E_g}\right] \tag{14}$$

3.4 Ionized-Impurity Screening

When sufficiently low temperatures and heavy doping conditions prevail, the bulk electron mobility is determined entirely by scattering from ionized impurities, which are described by the screened Coulomb potential energy function.

$$\vartheta = qe^{-\beta r} / 4\pi\varepsilon_s r \tag{15}$$

The charge on the ionized impurity is q and the screening length is $1/\beta$. The static dielectric permittivity is ε_S and r is the distance measured from the ionized impurity. In general, whether conditions are degenerate or non-degenerate, the screening length $1/\beta$ is calculated from β where[3]

$$\beta^2 = \frac{e^2}{\varepsilon_s \kappa T} \int \left(\frac{k}{\pi}\right)^2 f(1-f)\,dk \tag{16}$$

For non-degenerate conditions $f<<1$ and the reciprocal of β is equal to the classical Debye length, which is used to describe screening of ions in liquid electrolytes and in gaseous plasmas, as well as ionized-impurity screening in low-doped semiconductors.

$$\beta^2 = \frac{e^2}{\varepsilon_s \kappa T} \int \left(\frac{k}{\pi}\right)^2 f\,dk = \frac{ne^2}{\varepsilon_s \kappa T} = 1/\lambda_{Debye}^2 \tag{17}$$

$$\lambda_{Debye} = \sqrt{\varepsilon_s \kappa T / ne^2} \tag{18}$$

On the other hand, for degenerate conditions f is essentially equal to unity for energies less than the Fermi Level and a more sophisticated analysis must be carried out to derive the screening length for non-parabolic and degenerate conditions, which has been given by Rode and Cetnar.[6]

$$\beta_{RC}^2 = \frac{e^2(2m)^{3/2}}{2\pi^2\varepsilon_s\hbar^3} \cdot \left[E_F + E_g m/2m^* - \sqrt{(E_F + E_g m/2m^*)^2 - E_F(E_F+E_g)}\right]^{1/2} \times \left[1 - \frac{(m/m^* - 1)E_g/2}{\sqrt{(E_F + E_g m/2m^*)^2 - E_F(E_F+E_g)}}\right] \tag{19}$$

By way of comparison to classical work by Thomas and Fermi on this subject, who used degenerate and *parabolic* bands, their β_{TF} can be calculated from the formula[7]

$$\beta_{TF}^2 = \frac{4e^2 m^* k_F}{\varepsilon_s h^2} \tag{20}$$

In the parabolic band limit of large energy gap, eq. (19) for Rode-Cetnar screening must give results identical to those for the Thomas-Fermi screening of eq. (20). To prove that this is so, in eq. (19) set

$$\beta_{RC}^2 = \frac{e^2(2m)^{3/2}}{2\pi^2\varepsilon_s\hbar^3}\cdot\left["A"\right]^{1/2}\times\left["B"\right] \tag{21}$$

where

$$"A" = E_F + E_g m/2m^* - \sqrt{(E_F + E_g m/2m^*)^2 - E_F(E_F + E_g)} \tag{22}$$

and

$$"B" = 1 - \frac{(m/m^* - 1)E_g/2}{\sqrt{(E_F + E_g m/2m^*)^2 - E_F(E_F + E_g)}} \tag{23}$$

As the energy gap E_g approaches infinity,

$$\begin{aligned} "A" &\to (E_F + E_g m/2m^*)[1 - \sqrt{1 - E_F(E_F + E_g)/(E_F + E_g m/2m^*)^2}] \\ "A" &\to (E_F + E_g m/2m^*)[1 - 1 + E_F(E_F + E_g)/2(E_F + E_g m/2m^*)^2] \\ "A" &\to (E_F + E_g m/2m^*)E_F(E_F + E_g)/2(E_F + E_g m/2m^*)^2 \\ "A" &\to E_F m^*/m \end{aligned} \tag{24}$$

and

$$\begin{aligned} "B" &\to 1 - (m/m^* - 1)E_g/2/(E_g m/2m^*) \\ "B" &\to 1 - 2m^*(m/m^* - 1)/2m \\ "B" &\to 1 - 2m^*(m/m^* - 1)/2m \\ "B" &\to m^*/m \end{aligned} \tag{25}$$

Therefore,

$$\beta_{RC}^2 \to \frac{e^2(2m)^{3/2}}{2\pi^2\varepsilon_s\hbar^3}\cdot(m^*/m)^{3/2}\cdot E_F^{1/2}$$

$$\beta_{RC}^2 \to \frac{e^2(2m^*)^{3/2}\hbar k_F}{2\pi^2\varepsilon_s\hbar^3(2m^*)^{1/2}}$$

$$\beta_{RC}^2 \to \frac{m^* e^2 k_F}{\pi^2\varepsilon_s\hbar^2}$$

$$\beta_{RC}^2 \to \beta_{TF}^2 = \frac{4m^* e^2 k_F}{\varepsilon_s h^2} \tag{26}$$

Thus, Rode-Cetnar screening is identical to Thomas-Fermi screening in the limit of parabolic bands.

Some typical results for Thomas-Fermi and Rode-Cetnar screening lengths squared are shown in Figure 3 for degenerate ZnO. (Screening length is squared because only the reciprocal of the screening length squared appears in the formulas of Ref. 1.) Clearly, over the range of electron concentrations shown, the Rode-Cetnar theory is preferred over the Thomas-Fermi theory in order to achieve precision better than 5%. Obviously, for metals and metal alloys where electron concentrations are in the neighborhood of 10^{23}/cc it is essential to use Rode-Cetnar screening because the squared screening lengths differ by a factor of two.[8]

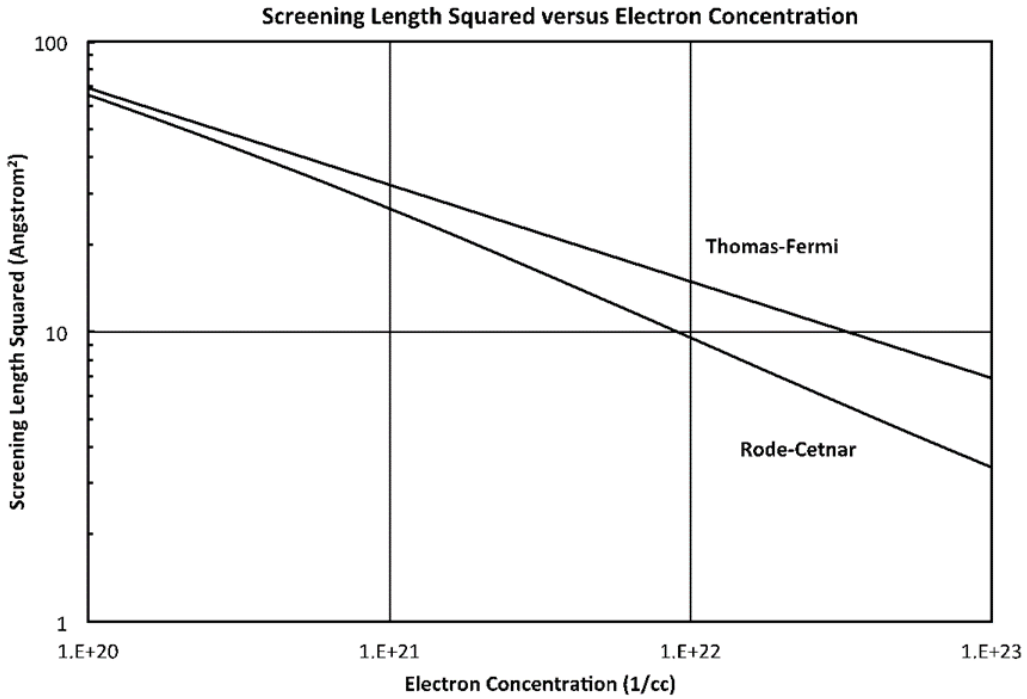

Figure 3: Squared Screening Lengths Calculated for Degenerately Doped ZnO at Low Temperature

Deviations between Thomas-Fermi theory and Rode-Cetnar theory in excess of 5% appear for electron concentrations greater than 10^{20}/cc, reaching more than 100% at 10^{23}/cc.

So, in conclusion, it is shown that eq. (19) exhibits correct behavior in the parabolic-band limit. However, this does not prove that eq. (19) is correct when the bands are *not* parabolic. To do this, the general equation (16) can be integrated numerically and compared to results calculated from eq. (19). This constitutes the last method of verification of eq. (19). Results are shown in Table 1.

Results for numerical integration of eq. (16) are compared to the Rode-Cetnar results from eq. (19) in the second and third columns of Table 1. The last column shows agreement between these two methods of calculation to lie within 100 ppm, or 0.01%. This result is consistent with the use of 500 integration intervals for the numerical calculation shown in Figure 4.

Table 1. Numerical Integration compared to Rode-Cetnar Results

Electron Concentration n[1/cc]	Numerical Integration BetaF^2[1/m^2]	R-C Formula BetaF^2[1/m^2]	Error (ppm)
1.00E+20	1.5257E+18	1.5258E+18	-7.038E+01
1.00E+21	3.7618E+18	3.7620E+18	-5.245E+01
1.00E+22	1.0487E+19	1.0488E+19	-5.195E+01
1.00E+23	2.9386E+19	2.9387E+19	-5.192E+01

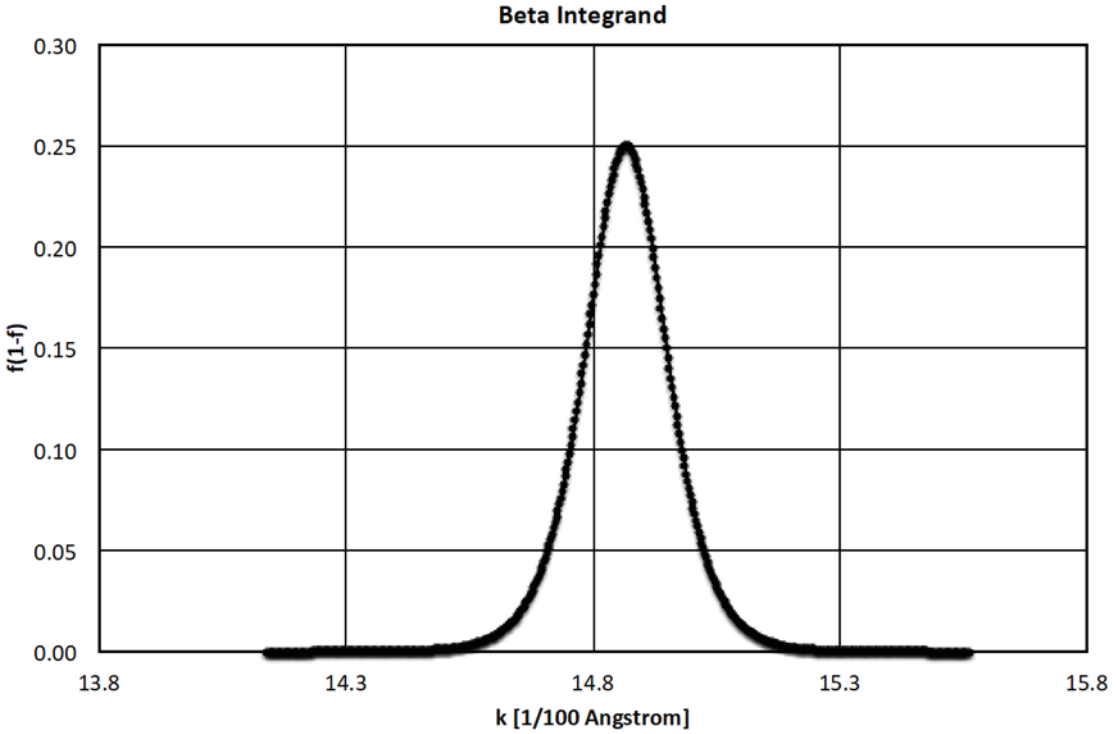

Figure 4: Numerical Integration of eq. (16) using 500 Equal Integration Intervals to Represent the Integrand *f(1-f)*

The integrand is plotted versus momentum k centered about the Fermi momentum (kF = 14.9 per 100 Angstroms) spanning energy from the Fermi level EF ±13κT. For this case EF/ κT = 140, T = 20K, and n = 1.11x10^{20}/cc.

Therefore, in conclusion, it is demonstrated that eq. (19) accurately describes ionized- impurity screening in degenerate semiconductors with non-parabolic bands.

3.5 Electron Mobility Due To Ionized-Impurity Scattering

The objective of this section is to verify the accuracy of the equation for electron mobility for degenerate conditions, in the limit of *parabolic* bands. When sufficiently low temperatures and heavy doping conditions prevail, the bulk electron mobility is determined practically entirely by scattering from ionized impurities.

In general, whether or not degeneracy prevails, electron drift mobility μ_d is given by the perturbation function g of the electron probability distribution under the influence of a weak electric field of strength F, generally less than about 100 V/cm at room temperature. Electron mobility is denoted by μii to signify the ionized-impurity mechanism when it is dominant. Including a non-parabolic conduction band, the electron drift mobility is given by[3]

$$\mu_d = \frac{\hbar}{3m} \cdot \frac{\int k^3 (g/Fd)\, dk}{\int k^2 f\, dk} \tag{27}$$

The reduced Planck constant is $\hbar$. If only ionized-impurity scattering is considered, the perturbation g is given by

$$g = -(eF/\hbar \nu_{ii}) \cdot \partial f / \partial k \tag{28}$$

Conduction band non-parabolicity is accounted for by the Jacobian quantity d.

$$1/d = 1 + (m/m^* - 1)/\sqrt{1 + 2\hbar^2 k^2 (m/m^* - 1)/mE_g} \tag{29}$$

The electron scattering rate due to ionized impurities is ν_{ii}. The electron drift mobility due to ionized-impurity scattering is thus given as

$$\mu_{ii} = -\frac{e}{3m} \cdot \frac{\int (k^3/\nu_{ii} d)(\partial f/\partial k)\, dk}{\int k^2 f\, dk} \tag{30}$$

In order to carry out the integral, note that the integrand takes on the behavior of a Dirac Delta function under highly degenerate conditions, as shown in Figure 5.

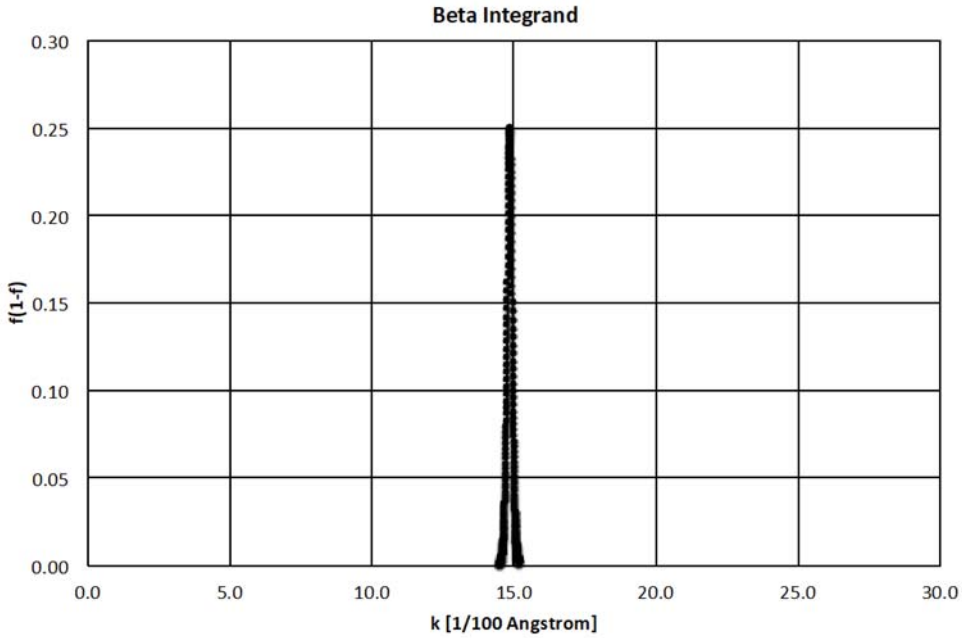

Figure 5: Data of Figure 4 is Plotted without using a Suppressed Zero for the Momentum

When the integrand *f(1-f)* of eq.(16) is plotted versus momentum without a suppressed zero for momentum, it is evident that *f(1-f)* approaches the behavior of a Dirac Delta function. In this case of high degeneracy, the electron scattering rate and the Jacobian *d*, set equal to d_F, can be removed from the integral, and the drift mobility is written as

$$\mu_{ii} = -\frac{e}{3m\nu_{ii}d_F} \cdot \frac{\int k^3(\partial f / \partial k)dk}{\int k^2 f\, dk} \tag{31}$$

The integral can be carried out using integration by parts.

$$\int k^3(\partial f / \partial k)dk = k^3 f - 3\int k^2 f\, dk \tag{32}$$

The first term on the right vanishes due to the upper and lower limits where *f* or *k* vanish, and eq. (11) is used to cancel the remaining integral term. Thus,

$$\mu_{ii} = \frac{e}{md_F\nu_{ii}} \tag{33}$$

The electron scattering rate due to ionized-impurities is evaluated at the Fermi level, denoted by subscript *F*.

$$\nu_{ii} = \frac{e^4 N m d_F}{8\pi\varepsilon_s^2\hbar^3 k_F^3} \cdot [D_F \cdot \ln(1+4k_F^2/\beta_F^2) - B_F] \tag{34}$$

The concentration of ionized scattering centers (impurities) is N, properly weighted for singly ionized and multiply ionized impurities. The D_F and B_F coefficients are given by

$$D_F = 1 + (2\beta_F^2 c_F^2 / k_F^2) + (3\beta_F^4 c_F^4 / 4k_F^4) \tag{35}$$

and

$$B_F = [4k_F^2/\beta_F^2 + 8(1 + 2k_F^2/\beta_F^2)c_F^2 + 6(1 + \beta_F^2/2k_F^2 - 4k_F^2/3\beta_F^2)c_F^4]/ (1 + 4k_F^2/\beta_F^2) \tag{36}$$

Wave function admixture and conduction band non-parabolicity are accounted for by the c and d quantities. See eqs. (8) and (29).

Since the objective of this section is to verify the accuracy of the equation for electron mobility for degenerate conditions in the limit of *parabolic* bands, let the energy gap approach infinity so c_F vanishes, $d_F = m^*/m$, $\beta_F = \beta_{TF}$ becomes the Thomas-Fermi value, and

$$D_F \to 1 \tag{37}$$

and

$$B_F \to 1/(1 + \beta_{TF}^2/4k_F^2) \tag{38}$$

The electron scattering rate due to ionized impurities becomes

$$\nu_{ii} = \frac{e^4 N m^*}{8\pi\varepsilon_s^2 \hbar^3 k_F^3} \cdot [\ln(1 + 4k_F^2/\beta_{TF}^2) - 1/(1 + \beta_{TF}^2/4k_F^2)] \tag{39}$$

and the electron mobility becomes

$$\mu_{ii} = e/m^* \nu_{ii} \tag{40}$$

Therefore, the degenerate electron mobility due to ionized impurities in the parabolic limit becomes

$$\mu_{ii} = \frac{8\pi\varepsilon_s^2 \hbar^3 k_F^3}{e^3 N m^{*2}} / [\ln(1 + 4k_F^2/\beta_{TF}^2) - 1/(1 + \beta_{TF}^2/4k_F^2)] \tag{41}$$

This can be expressed more simply as

$$\mu_{ii} = \frac{3\varepsilon_s^2 h^3 n}{e^3 m^{*2} N} / [\ln(1 + 4k_F^2/\beta_{TF}^2) - 1/(1 + \beta_{TF}^2/4k_F^2)] \tag{42}$$

In the limit of parabolic bands, the electron mobility due to ionized impurities as given by eqs. (41) and (42) must agree with the expression given by Look *et al.* in their eq. (1), which, when adapted to the present notation is[4]

$$\mu_{ii}^{DCL} = \frac{24\pi^3 \varepsilon_s^2 \hbar^3 n}{e^3 m^{*2} N} / [\ln(1+4k_F^2/\beta_{TF}^2) - 1/(1+\beta_{TF}^2/4k_F^2)] \tag{43}$$

However, the pre-factor $3h^3 = 24\pi^3\hbar^3$ and, hence, eqs. (41) and (42) are identical with eq. (43): *Q.E.D.*

Therefore, in every case examined, the earlier formulas,[1] which were developed for degenerate non-parabolic bands, converge properly in the parabolic limit to the exact same results as are known for parabolic bands. This successfully completes the major objective of this work.

4. Acknowledgments

Supported by the Air Force Office of Scientific Research under project FA9550-17RYCOR490.
This work would not have been possible without encouragement and advice from John S. Cetnar.
It is a pleasure to acknowledge helpful suggestions from David C. Look.

5. References

1. Daniel L. Rode, Phase I Final Report 181026 for AFRL, "Electron Mobility of Degenerate Semiconductors Due To Ionized-Impurity Scattering" (October 2018)
2. E. O. Kane, "Semiconductors and Semimetals" 1 (Academic Press, New York, 1966), Ch. 3
3. D. L. Rode, "Semiconductors and Semimetals" 15 (Academic Press, New York, 1975), Ch. 1
4. D. C. Look and K. D. Leedy, Proc. SPIE 8263 826302-9 (2012)
5. D. C. Look, K. D. Leedy, L. Vines, B. G. Svensson, A. Zubiaga, F. Tuomisto, D.
6. R. Doutt, and L. J. Brillson, Phys. Rev. B84 115202 (2011), Fig. 1
7. John S. Cetnar and D. L. Rode, "Fermi Level and Electrostatic Screening Factor in Degenerate Semiconductors and Metal Alloys," J. Electron. Materials 48(5), 3399- 3404 (March 2019)
8. C. Kittell, "Introduction to Solid-State Physics," 7th ed. (John Wiley & Sons, NY,
9. 1996), p.281
10. D. L. Rode and J. S. Cetnar, "Electrical Resistivity of Cu-Au Metal Alloys" (unpublished)

Appendix A: Effective Mass

The concept of mass can be problematical, especially for considerations in solid-state physics. Classically, there are two kinds of mass: what Einstein called inertial mass and ponderable mass. He demonstrated in his discussions of Relativity Theory that these two masses are necessarily equal to one another for Galilean systems. Their defining equations are

$$W = gm \tag{A1}$$

$$F = ma \tag{A2}$$

In these cases W is weight, F is force, and m is mass, the same in either case according to Einstein; g and a are the gravitational acceleration and the inertial acceleration. Eq. (A2) naturally leads to the mass used in the kinetic energy formula, eq. (1).

$$K.E. = mv^2/2 = p^2/2m \tag{A3}$$

In the case of semiconductor problems of present interest, we may speak of a mass associated with kinetic energy, so that

$$E = \hbar^2 k^2/2m^* = p^2/2m^* \tag{A4}$$

But, it must be kept in mind that this is meaningful *only* for parabolic bands, in which case the effective mass m^* is constant for all energies.

Of course, it is not true that the bands are parabolic for all energies (and that the effective mass m^* is constant) (see Figure 1). Instead, it is wiser to use the actual dispersion relation $E(k)$, which relates energy and momentum as given by eq. (3), for electron transport theory. Indeed, Heisenberg showed that energy and momentum, along with time and distance coordinates are canonical variables, and therefore it makes sense to use the dispersion relation $E(k)$ and to dispense with the idea of "mass" altogether.

Nevertheless, it is a great temptation to "simplify" and so the questionable idea of "effective mass" has been popularized. However, it is unclear how to define "effective mass" – should it be in terms of the kinetic energy, or should it relate to the density-of-states [involving the second derivative of $E(k)$], or should it signify the group velocity [involving the first derivative of $E(k)$], or perhaps the mass related to Newton's Law in eq. (A2)?

Although it is not a strictly proper answer to the above objections, consider the quantity $1/d_F$ of eq. (29), which in the limit of parabolic bands equals $m^*/m = 0.34$ for the present work relating to ZnO. We may compare $1/d_F$ to the effective mass $m^*(n)$ formula proposed by Look and Leedy.[4]

$$m^*(n) = \frac{m^*(n=0)}{1 - E_F[1 - m^*(n=0)/m]^2 / E_g} \tag{A5}$$

By direct calculation, when the electron concentration is below 5×10^{20}/cc, eq. (A5) agrees with $1/d_F$ to within 5%, but when $n = 5 \times 10^{21}$/cc, eq.(A5) disagrees with $1/d_F$ by 16%. For larger values of n, eq. (A5) fails insofar as it yields negative effective mass values for n somewhat greater than 2×10^{22}/cc. Therefore, for the range of electron concentration considered by Look and Leedy, i.e. 1×10^{20} to 2×10^{21}/cc, their eq. (A5) is accurate to within about 10%.

Appendix B: Effects of Non-Parabolicity and Wave Function Admixture

Band non-parabolicity and wave function admixture exhibit opposite effects on electron mobility. Non-parabolicity causes the calculated mobility to *decrease* due to increased apparent density-of-states effective mass and increased electron scattering rate. Wave function admixture causes it to *increase* due to reduced scattering rate because the *s* and *p* basis functions are orthogonal. The effects are shown quantitatively in the following table.

Table B-1. Effects of Non-parabolicity and Wave Function Admixture

n[1/cc]=	1.00E+21	
mu- ii[cm^2/V/s]	64.96	**effect[%]**
parabolic mu-ii	68.81	5.9
s-function mu-ii	52.21	-19.6
n[1/cc]=	5.00E+21	
mu- ii[cm^2/V/s]	43.90	**effect[%]**
parabolic mu-ii	53.50	21.9
s-function mu-ii	30.64	-30.2

In the table, parabolic mobility is calculated by assuming the energy gap equals infinity. The *s*-function mobility is calculated by setting c^2 equal to zero. Therefore, since c^2 equals zero for parabolic bands, the parabolic mobility includes both non- parabolicity corrections and admixture corrections.